

**Electronic Supplementary Information for
Design and Synthesis of Mixed-Ligand Architectured Zn-based Coordination
Polymers for Energy Storage**

Tapan Kumar Ghosh and G Ranga Rao*

Department of Chemistry and DST-Solar Energy Harnessing Centre (DSEHC), Indian Institute of Technology Madras, Chennai-600036, India

*Corresponding author; E-mail: grrao@iitm.ac.in

Table S1 Crystallographic data and structure refinement parameters of Zn-CP

Identification code	Zn-CP (NIZN)
Empirical formula	C ₁₉ H ₂₀ N ₂ O ₁₀ Zn
Formula weight	501.74
Temperature	296(2) K
Crystal system	Monoclinic
Space group	C2/c
<i>a</i> (Å)	7.87050(10)
<i>b</i> (Å)	17.3418(3)
<i>c</i> (Å)	32.3764(5)
α (deg)	90
β (deg)	92.492(4)
γ (deg)	90
Wavelength (Å)	0.71073
Volume (Å ³)	4414.83(12)
<i>Z</i>	8
ρ_{calcd} (mg m ⁻³)	1.510
μ (mm ⁻¹)	1.170
<i>F</i> (000)	2064
Crystal size (mm ³)	0.200 × 0.180 × 0.150
θ range for data collection (deg)	2.844 to 24.998°
Index ranges	-9 ≤ <i>h</i> ≤ 9, -20 ≤ <i>k</i> ≤ 20, -38 ≤ <i>l</i> ≤ 38
Reflections collected	27833
Independent reflections	3896 ($R_{\text{int}} = 0.0519$)
Absorption correction	Semi-empirical from equivalents
Max. and min. transmission	0.7453 and 0.6235
Refinement method	Full-matrix least-squares on <i>F</i> ²
Data/restraints/parameters	3896/12/310
Goodness-of-fit on <i>F</i> ²	1.204
R_1^a , wR_2^b [<i>I</i> > 2σ(<i>I</i>)]	$R_I = 0.0693$, $wR_2 = 0.1751$
R_1^a , wR_2^b (all data)	$R_I = 0.0760$, $wR_2 = 0.1799$
Largest diff. peak and hole (e Å ⁻³)	0.880 and -0.589
$^a R_1 = \sum (F_o - F_c) / \sum F_o \quad ^b R_2 = \left[\sum \left\{ w(F_o^2 - F_c^2)^2 \right\} / \sum \left\{ w(F_o^2)^2 \right\} \right]^{1/2}$	

Table S2 Bond lengths (\AA) and angles ($^\circ$) for Zn-CP.

Zn(1)-O(1)	1.928(4)
Zn(1)-O(3)#1	1.935(3)
Zn(1)-N(1)	2.026(4)
Zn(1)-O(7)	2.065(5)
C(1)-O(2)	1.232(6)
C(1)-O(1)	1.279(6)
C(1)-C(2)	1.498(7)
C(2)-C(3)	1.385(7)
C(2)-C(7)	1.393(7)
C(3)-C(4)	1.390(7)
C(3)-H(3)	0.9300
C(4)-C(5)	1.390(7)
C(4)-C(9)	1.500(7)
C(5)-C(6)	1.386(7)
C(5)-H(5)	0.9300
C(6)-C(7)	1.386(7)
C(6)-C(8)	1.494(7)
C(7)-H(7)	0.9300
C(8)-O(6)	1.230(7)
C(8)-O(5)	1.291(7)
C(9)-O(4)	1.237(6)
C(9)-O(3)	1.269(6)
C(10)-N(1)	1.337(7)
C(10)-C(11)	1.370(8)
C(10)-H(10)	0.9300
C(11)-C(12)	1.388(8)
C(11)-H(11)	0.9300
C(12)-C(13)	1.395(8)
C(12)-C(15)	1.486(7)
C(13)-C(14)	1.366(7)
C(13)-H(13)	0.9300
C(14)-N(1)	1.340(7)

C(14)-H(14)	0.9300
C(15)-C(16)	1.365(9)
C(15)-C(19)	1.377(8)
C(16)-C(17)	1.376(10)
C(16)-H(16)	0.9300
C(17)-N(2)	1.297(10)
C(17)-H(17)	0.9300
C(18)-N(2)	1.303(9)
C(18)-C(19)	1.376(8)
C(18)-H(18)	0.9300
C(19)-H(19)	0.9300
N(2)-H(2A)	0.86(2)
O(7)-H(7A)	0.85(2)
O(7)-H(7B)	0.839(19)
O(8)-H(8B)	0.85(2)
O(8)-H(8A)	0.86(2)
O(9)-H(9A)	0.84(2)
O(9)-H(9B)	0.85(2)
O(1)-Zn(1)-O(3)#1	119.59(15)
O(1)-Zn(1)-N(1)	127.79(17)
O(3)#1-Zn(1)-N(1)	103.91(16)
O(1)-Zn(1)-O(7)	104.39(18)
O(3)#1-Zn(1)-O(7)	98.89(17)
N(1)-Zn(1)-O(7)	95.25(19)
O(2)-C(1)-O(1)	123.7(5)
O(2)-C(1)-C(2)	121.1(4)
O(1)-C(1)-C(2)	115.3(4)
C(3)-C(2)-C(7)	119.5(5)
C(3)-C(2)-C(1)	120.6(4)
C(7)-C(2)-C(1)	119.9(4)
C(2)-C(3)-C(4)	120.5(4)
C(2)-C(3)-H(3)	119.7
C(4)-C(3)-H(3)	119.7
C(5)-C(4)-C(3)	119.4(4)
C(5)-C(4)-C(9)	120.6(4)

C(3)-C(4)-C(9)	119.8(4)
C(6)-C(5)-C(4)	120.5(5)
C(6)-C(5)-H(5)	119.8
C(4)-C(5)-H(5)	119.8
C(7)-C(6)-C(5)	119.7(5)
C(7)-C(6)-C(8)	118.7(5)
C(5)-C(6)-C(8)	121.6(5)
C(6)-C(7)-C(2)	120.4(5)
C(6)-C(7)-H(7)	119.8
C(2)-C(7)-H(7)	119.8
O(6)-C(8)-O(5)	122.3(5)
O(6)-C(8)-C(6)	121.0(5)
O(5)-C(8)-C(6)	116.7(5)
O(4)-C(9)-O(3)	124.4(5)
O(4)-C(9)-C(4)	120.2(5)
O(3)-C(9)-C(4)	115.3(4)
N(1)-C(10)-C(11)	121.9(6)
N(1)-C(10)-H(10)	119.1
C(11)-C(10)-H(10)	119.1
C(10)-C(11)-C(12)	121.0(6)
C(10)-C(11)-H(11)	119.5
C(12)-C(11)-H(11)	119.5
C(11)-C(12)-C(13)	116.0(5)
C(11)-C(12)-C(15)	121.1(5)
C(13)-C(12)-C(15)	122.9(5)
C(14)-C(13)-C(12)	120.4(5)
C(14)-C(13)-H(13)	119.8
C(12)-C(13)-H(13)	119.8
N(1)-C(14)-C(13)	122.4(5)
N(1)-C(14)-H(14)	118.8
C(13)-C(14)-H(14)	118.8
C(16)-C(15)-C(19)	116.4(6)
C(16)-C(15)-C(12)	121.1(6)
C(19)-C(15)-C(12)	122.5(5)
C(15)-C(16)-C(17)	119.8(7)

C(15)-C(16)-H(16)	120.1
C(17)-C(16)-H(16)	120.1
N(2)-C(17)-C(16)	123.1(7)
N(2)-C(17)-H(17)	118.4
C(16)-C(17)-H(17)	118.4
N(2)-C(18)-C(19)	122.7(7)
N(2)-C(18)-H(18)	118.7
C(19)-C(18)-H(18)	118.7
C(18)-C(19)-C(15)	119.7(6)
C(18)-C(19)-H(19)	120.1
C(15)-C(19)-H(19)	120.1
C(10)-N(1)-C(14)	118.3(5)
C(10)-N(1)-Zn(1)	121.4(4)
C(14)-N(1)-Zn(1)	120.3(4)
C(17)-N(2)-C(18)	118.3(6)
C(17)-N(2)-H(2A)	114(5)
C(18)-N(2)-H(2A)	128(5)
C(1)-O(1)-Zn(1)	117.0(3)
C(9)-O(3)-Zn(1)#2	120.4(3)
Zn(1)-O(7)-H(7A)	103(5)
Zn(1)-O(7)-H(7B)	112(5)
H(7A)-O(7)-H(7B)	109(3)
H(8B)-O(8)-H(8A)	108(4)
H(9A)-O(9)-H(9B)	111(4)

Symmetry transformations used to generate equivalent atoms:

#1 x-1/2,y+1/2,z #2 x+1/2,y-1/2,z

Table S3 Selected hydrogen bond distances (\AA) and angles ($^\circ$) for Zn-coordination polymer (Zn-CP)

D–H…A type	D–H (\AA)	H…A (\AA)	D–H…A (\AA)	D–H…A ($^\circ$)
O(7)–H(7A)…O(2)	0.852	1.839	2.691	166.3
O(7)–H(7b)…O(9)	0.841	1.87	2.711	166.2
N(2)–H(2A)…O(5)	0.867	1.71	2.577	173.7
D = Donor, A = Acceptor				

Table S4 Comparison of supercapacitor performance of Zn-CP/rGO with previously reported MOFs/CPs and related composites.

Material	Linkers used	Synthesis conditions	C_s (F/g)	Rate	Electrolyte	C_s retention	Ref.
[Co(H ₂ O) ₂ (Fc(PHOO) ₂)·2H ₂ O] _n	Ferrocene and phosphonic acid	RT	2517	2 A g ⁻¹	1 M t-Bu ₃ PC ₁₀ H ₂₅ BF ₄	90% after 1000 cycles	[22]
Cu-Asp	L-Aspartic acid	RT	367	0.6 A g ⁻¹	2 M KOH	94% after 1000 cycles	[29]
CoNi-MOF	H ₂ BDC	120 °C (12 h)	1044	2 A g ⁻¹	1 M KOH		[30]
Co(II)-TMU-63# 30%CoMn ₂ O ₄ NCP	H ₂ tpa and dapz	105 °C (72 h)	1420	7 A g ⁻¹	2 M KOH	93.3% after 7000 cycles	[31]
{[Co(Hmt)(tfbdc)(H ₂ O) ₂]·(H ₂ O) ₂ } _n	HMT and H ₂ tfbdc	Volatilized at RT	2474	1 A g ⁻¹	1 M KOH	94.3% after 2000 cycles	[32]
Ni ₃₃ /ZIF-67/rGO ₂₀	2-MeIm	RT	304	1 A g ⁻¹	1 M H ₂ SO ₄	99% after 1000 cycles	[33]
rGO/Zn-MOF@PANI	H ₂ BDC	160 °C (5 h)	372	0.1 A g ⁻¹	1 M H ₂ SO ₄		[34]

Ce-MOF/CNT	H ₃ BTC	Ultrasonication, RT	129.6	1 A g ⁻¹	1 M KOH	85% after 5000 cycles	[35]
Ce-MOF/GO	H ₃ BTC	Ultrasonication, RT	233.8	1 A g ⁻¹	1 M KOH	86% after 5000 cycles	[35]
Cu- MOF/rGO	H ₄ L	Ultrasonication, RT	462	0.8 A g ⁻¹	1 M Na ₂ SO ₄	93.7% after 1000 cycles	[37]
Zn/Ni-MOF (MOF-2)	H ₂ BDC	100 °C (8 h)	1620	0.25 A g ⁻¹	6 M KOH	91% after 3000 cycles	[52]
GA/MOF (Fe ³⁺)	H ₂ BDC	Hydrothermal	389	0.5 A g ⁻¹	1 M H ₂ SO ₄	74.4% after 10000 cycles	[53]
CNTs@Mn- MOF	H ₂ BDC	Hydrothermal	203.1	1 A g ⁻¹	1 M Na ₂ SO ₄		[58]
ZIF-67/rGO	2-MeIm	Stirring, RT	562	5 mV s ⁻¹	1 M Na ₂ SO ₄ + 0.2 M K ₃ [Fe(CN) ₆	90% after 1000 cycles	[60]
rGO- HKAUST-1	H ₃ BTC	Hydrothermal	385	1 A g ⁻¹	0.5 M Na ₂ SO ₄		[S1]
ZIF-67	2-MeIm	Stirring, RT	188.7	1 A g ⁻¹	1 M KOH	105% after 3000 cycles	[S2]
POAP/Cu- bipy-BTC	2,2'-bpy and H ₃ BDC	Hydrothermal- electropolymeriz- ation	422	1 mA	0.1 M HClO ₄	93% after 1000 cycles	[S3]
Carbonized Zn- MOF/PANI	8- hydroxyqui- noline	in situ chemical oxidative polymerization	477	1 A g ⁻¹	1 M H ₂ SO ₄		[S4]
Co-MOF	FcDCA and 4,4'-bpy	Ultrasonication, RT	446.8	1.2 A g ⁻¹	1 M KOH	88.3% after 8000 cycles	[S5]
Na/Co-MOF	4,4'-Azpye and 2,5'- TDCA	Ultrasonication, RT	321.8	4 A g ⁻¹	0.5 M Na ₂ SO ₄	97.4% after 5000 cycles	[S6]
Zn-CP/rGO	4,4'-bpy and 1,3,5-BTC	Ultrasonication, RT	377	1 A g ⁻¹	2 M KOH	85% after 6000 cycles	This work

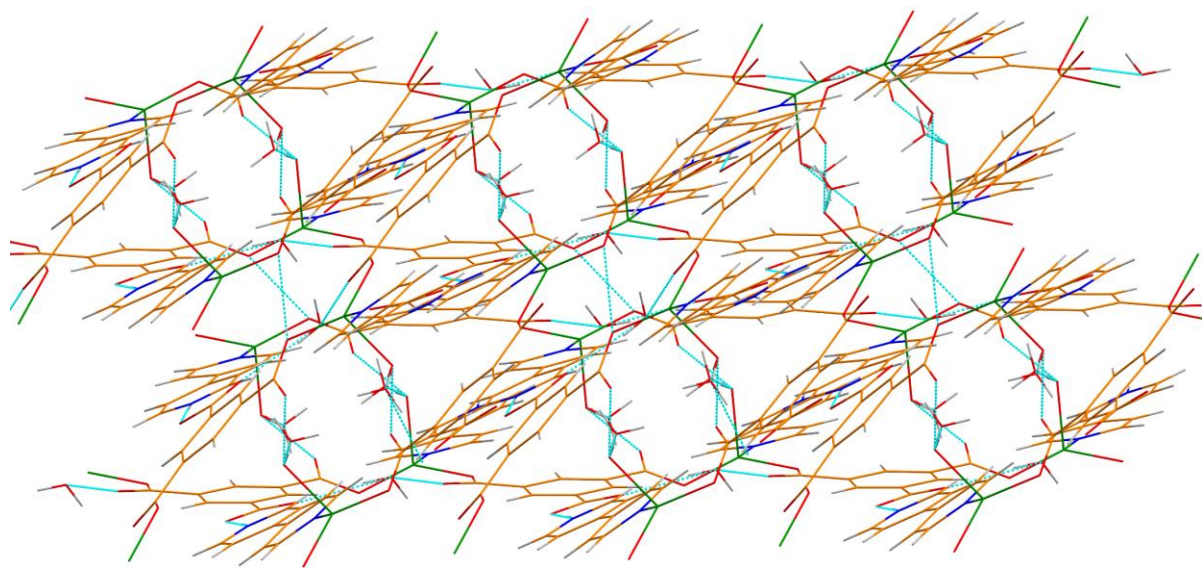


Fig. S1 3D wireframe structure of Zn-coordination polymer (Zn-CP).

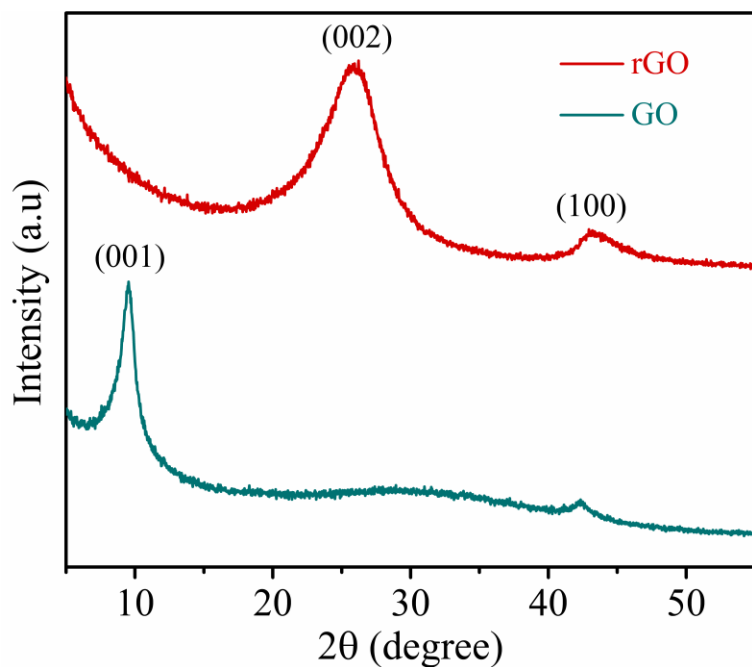


Fig. S2 Powder X-ray diffraction pattern of GO and rGO.

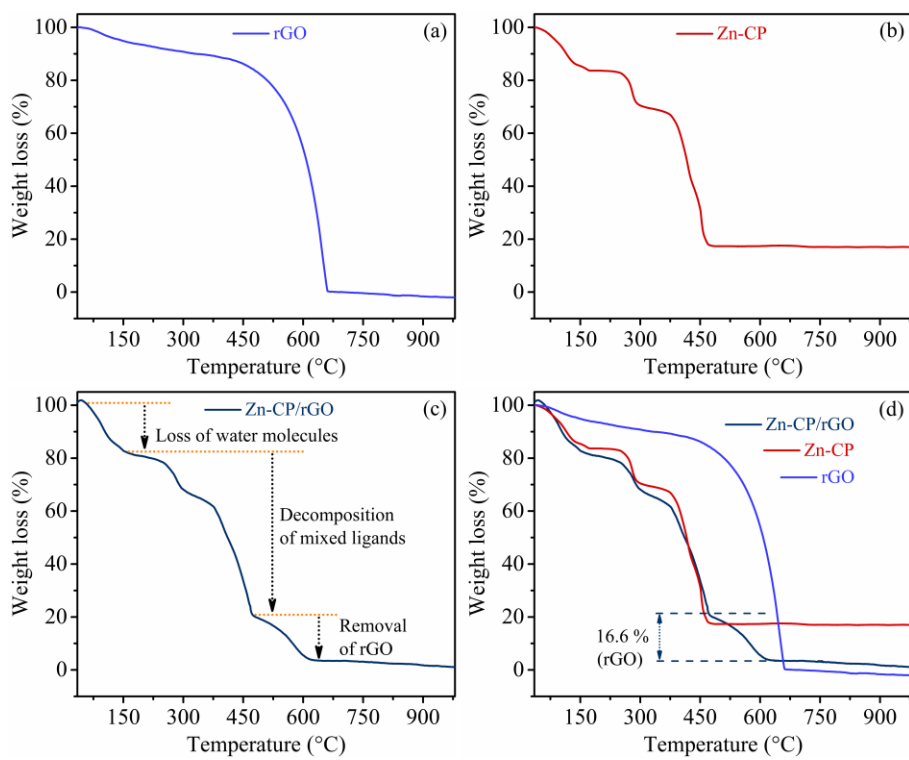


Fig. S3 TGA curves of (a) rGO, (b) Zn-CP, (c) Zn-CP/rGO and (d) comparative TGA.

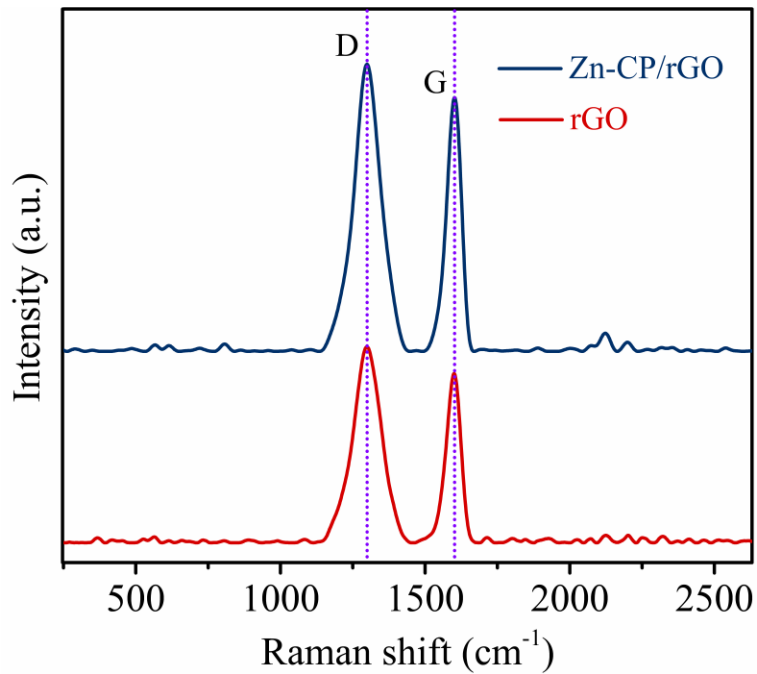


Fig. S4 Raman spectra of rGO and Zn-CP/rGO.

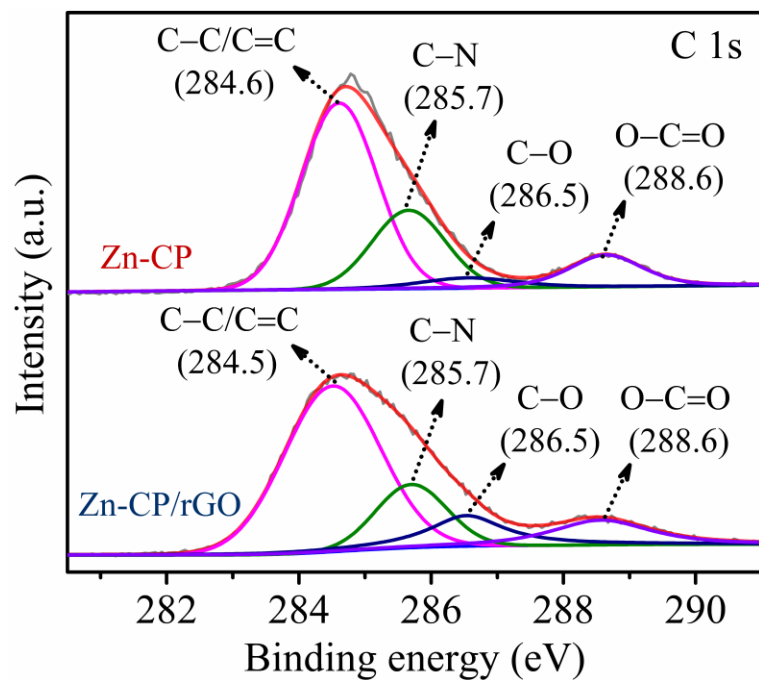


Fig. S5 High resolution deconvoluted C1s spectra of Zn-CP and Zn-CP/rGO samples.

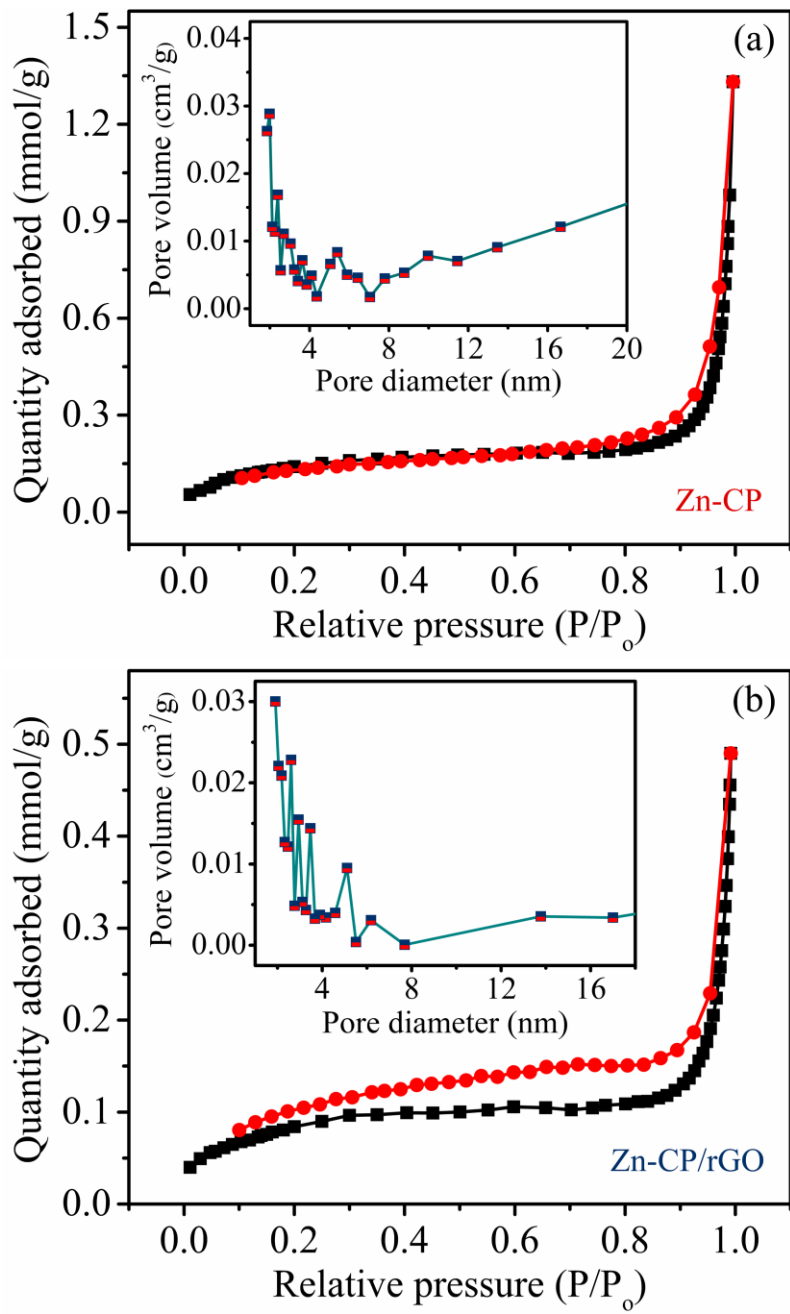


Fig. S6 N₂ adsorption-desorption isotherm of (a) Zn-CP and (b) Zn-CP/rGO (inset: BJH pore size distribution curves).

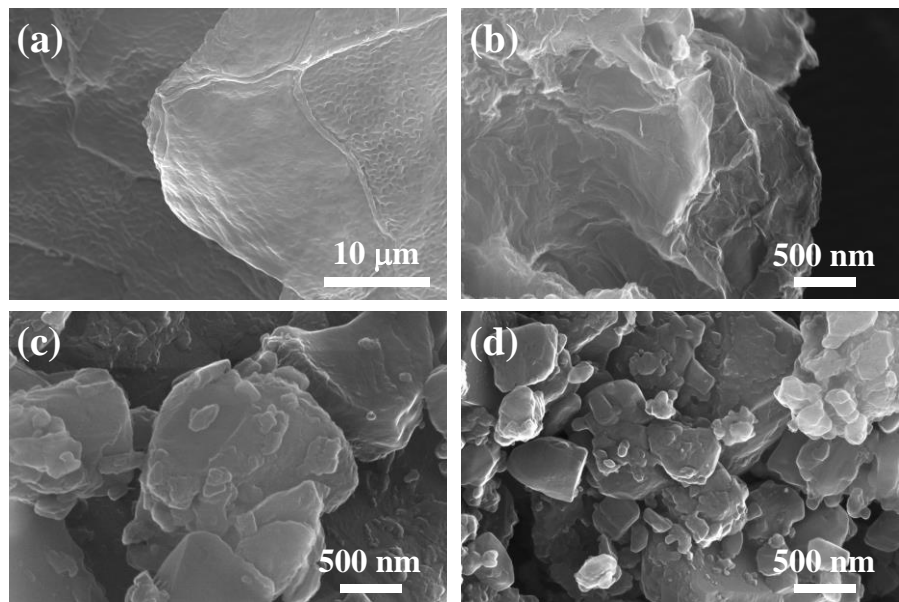


Fig. S7 FESEM images of (a, b) rGO, (c) Zn-CP and (d) Zn-CP/rGO.

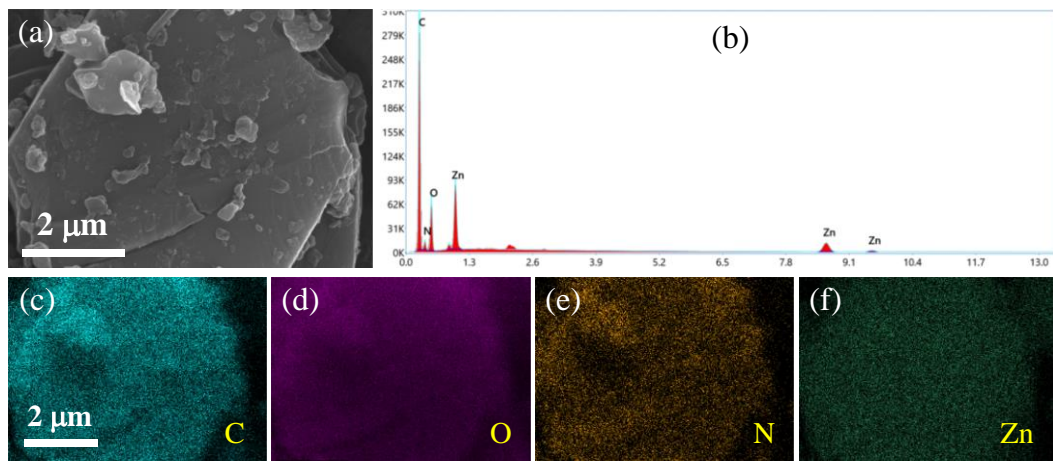


Fig. S8 (a) FESEM image from which elemental mapping was taken, (b) EDS measurement of Zn-CP showing different elements and (c-f) elemental mapping of Zn-CP.

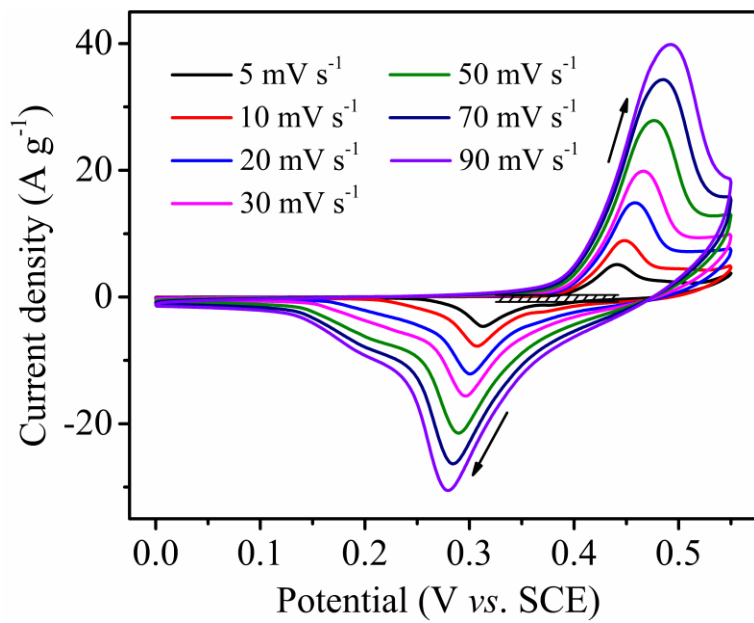


Fig. S9 CV profile of Zn-CP electrode measured at different scan rates.

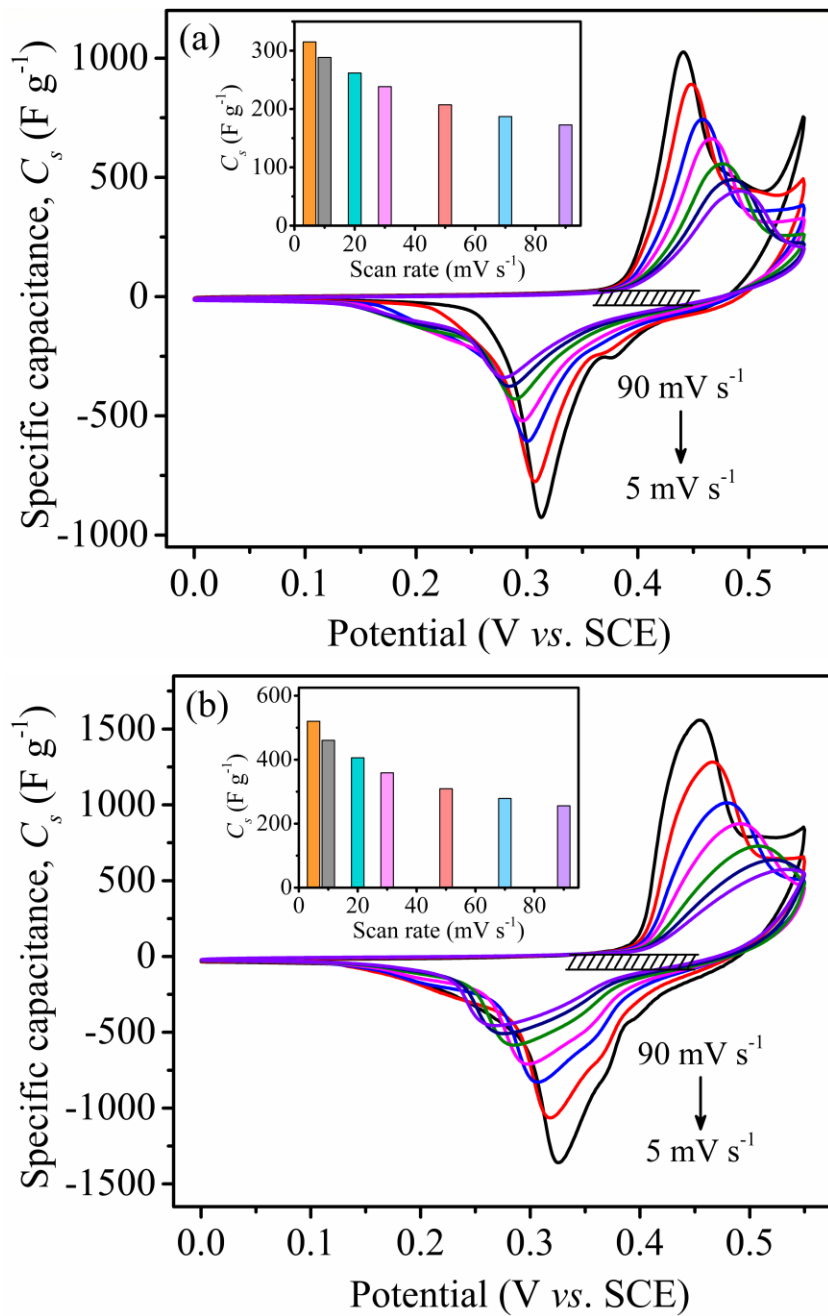


Fig. S10 Plot of specific capacitance vs applied potentials at different scan rates for (a) Zn-CP, and (b) Zn-CP/rGO electrodes; Inset shows the specific capacitance vs scan rate graph.

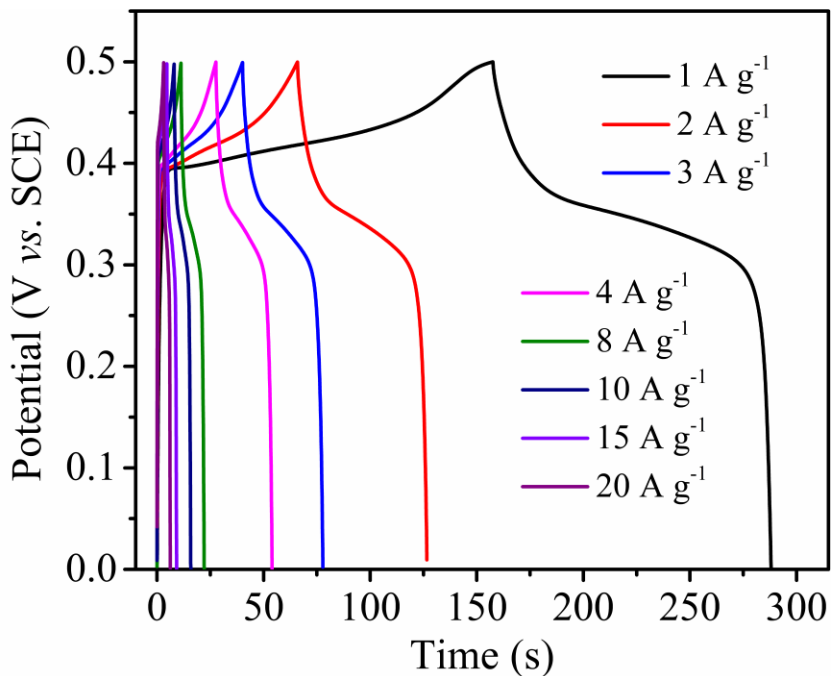


Fig. S11 GCD profile of Zn-CP electrode measured at different current densities.

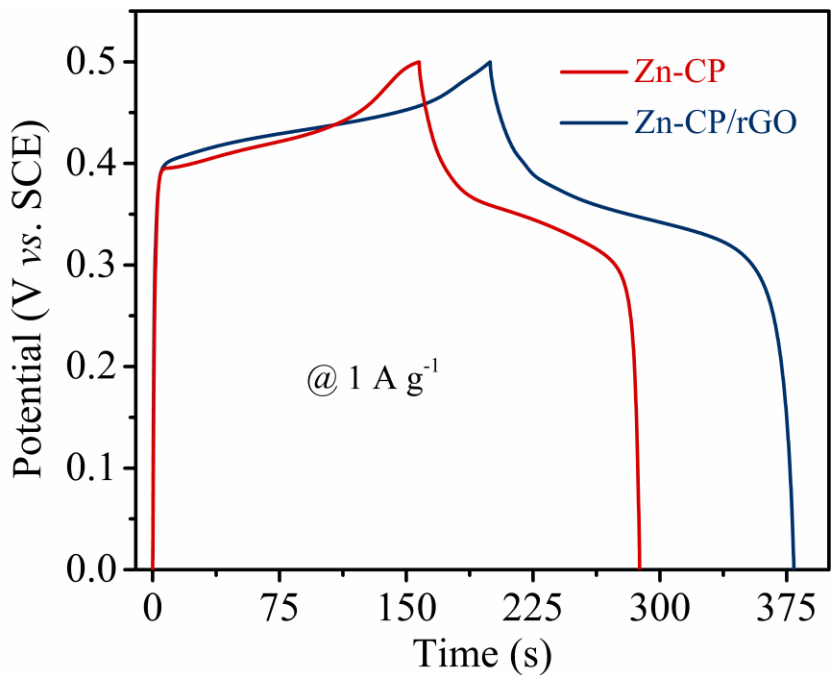


Fig. S12 Comparison of GCD profiles between Zn-CP and Zn-CP/rGO electrodes measured at a current density of 1 A g⁻¹.

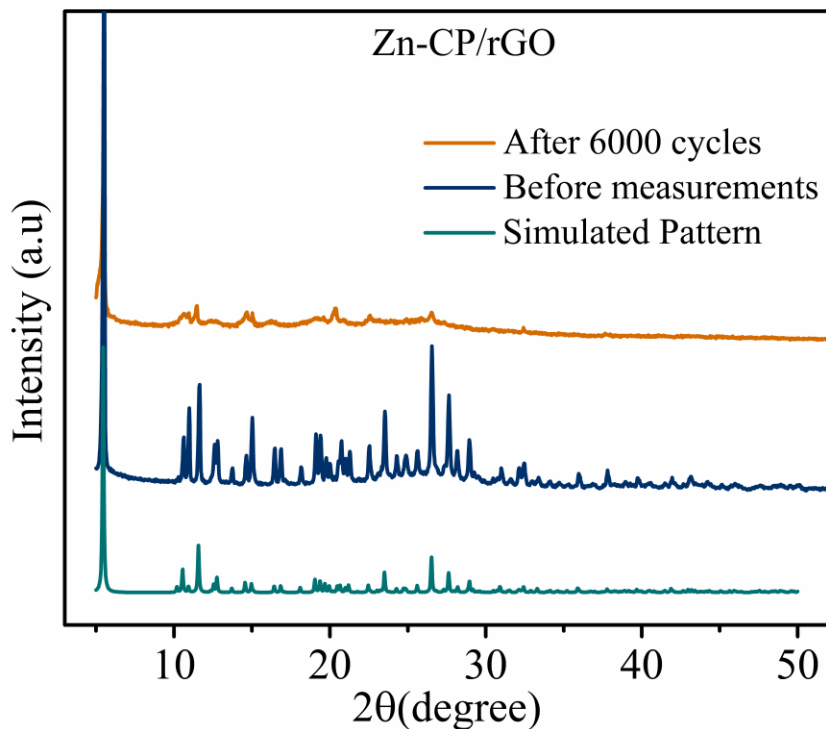


Fig. S13 The comparative PXRD pattern of Zn-CP/rGO electrode before and after cyclic measurements.

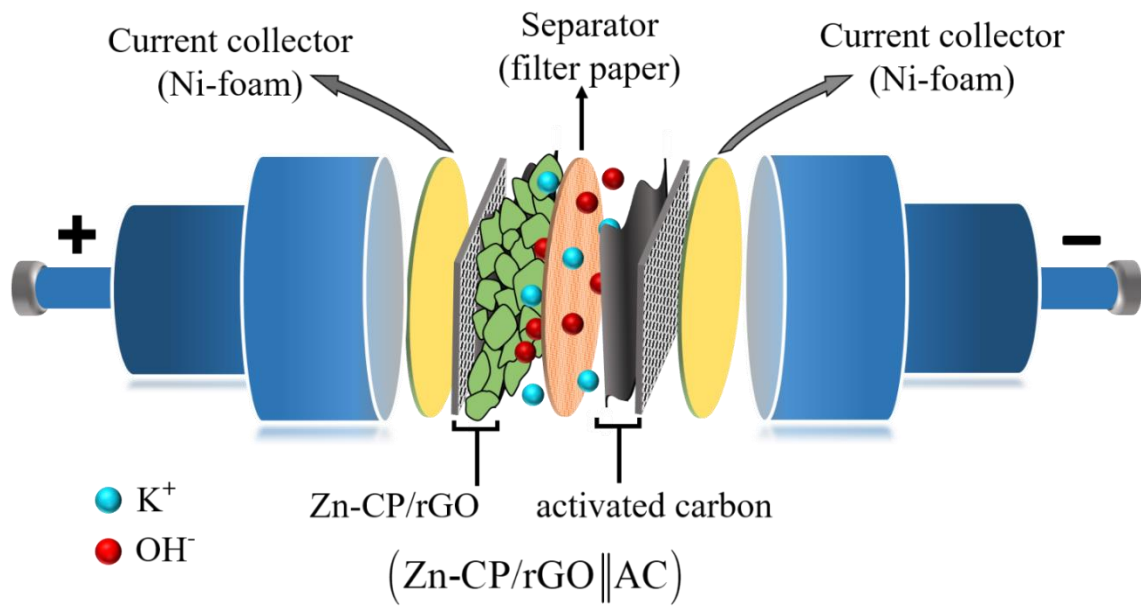


Fig. S14 Schematic representation of the hybrid supercapattery (HSC) device $Zn\text{-CP/rGO} \parallel AC$ assembled in a Swagelok cell using Zn-CP/rGO as positive and AC as negative electrodes.

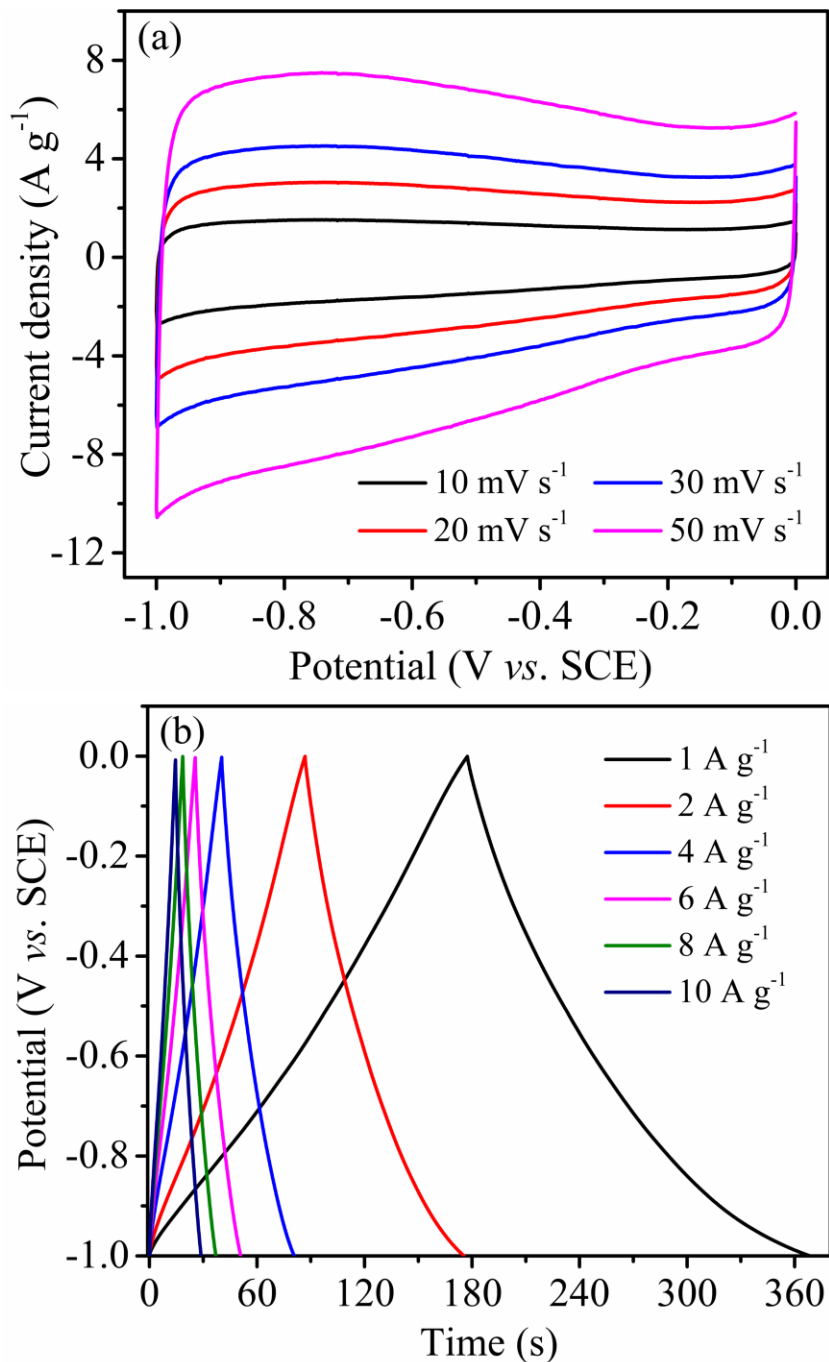


Fig. S15 (a) CV profile at different scan rates, and (b) GCD profile at different current densities of activated carbon (AC) measured using 2 M KOH electrolyte.

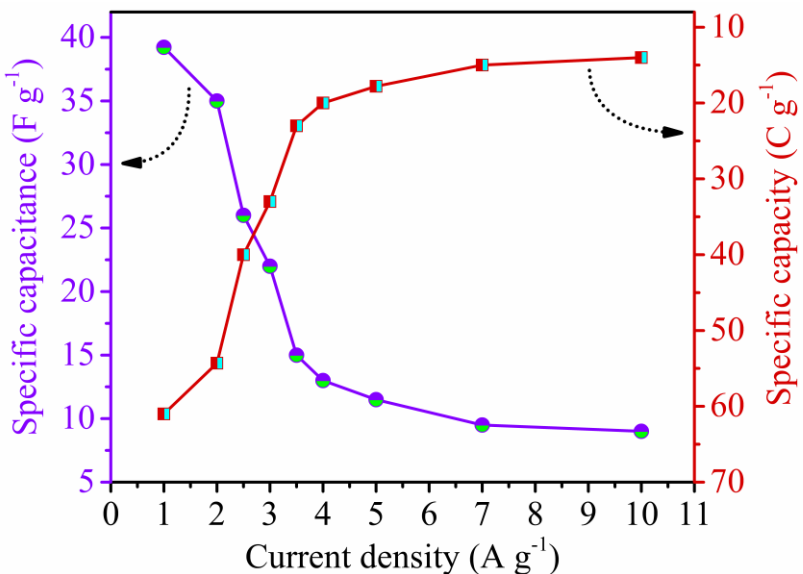


Fig. S16 Plot of specific capacitance and specific capacity vs current density of Zn-CP/rGO||AC HSC device.

References

- (1) P. Srimuk, S. Luanwuthi, A. Krittayavathananon and M. Sawangphruk, *Electrochim. Acta*, 2015, **157**, 69–77.
- (2) D. Zhang, H. Shi, R. Zhang, Z. Zhang, N. Wang, J. Li, B. Yuan, H. Bai and J. Zhang, *RSC Adv.*, 2015, **5**, 58772–58776.
- (3) A. Ehsani, J. Khodayari, M. Hadi, H. M. Shiri and H. Mostaanzadeh, *Ionics*, 2017, **23**, 131–138.
- (4) S. N. Guo, Y. Zhu, Y. Y. Yan, Y. Min, J. Fan, Q. Xu and H. Yun, *J. Power Sources*, 2016, **316**, 176–182.
- (5) R. Rajak, M. Saraf, A. Mohammad and S. M. Mobin, *J. Mater. Chem. A*, 2017, **5**, 17998–18011.
- (6) R. Rajak, M. Saraf and S. M. Mobin, *Inorg. Chem.*, 2020, **59**, 1642–1652.